

Effect of Sheet Thickness on Fatigue Behavior of Friction Stir Spot Weld of Al 6061-T6 Lap-shear Configuration

A.R. Shahani*, A. Farrahi

Mechanical Engineering Department, K.N. Toosi University of Technology, Tehran, Iran.

Article info

Article history:

Received 20 July 2018

Received in revised form

10 September 2018

Accepted 19 September 2018

Keywords:

Friction stir spot welding

Fatigue

Mechanical behavior

Sheet thickness

Abstract

The effect of three different sheet thicknesses of friction stir spot welding on lap-shear specimens of Al 6061-T6 alloy was experimentally analyzed. Different fatigue life evaluation models were applied to estimate the fatigue behavior of the friction stir spot welding in different thicknesses. Experimental results show a clear correlation between static strength and fatigue behavior of different welding conditions. Results of tensile and fatigue tests demonstrated the sheets with 2mm indicated the optimum thickness which were studied in this research. At the same cycles, fatigue results of different thicknesses showed considerable differences in the low cycles in comparison with the higher ones. The evaluation models of Pook, Zhang and three-dimensional finite element models were investigated in the different sheet thicknesses. The three-dimensional finite element model evaluated fatigue behavior better than the other models at different sheet thicknesses.

Nomenclature

k_I	Mode I local stress intensity factor	k_{II}	Mode II local stress intensity factor
α	Kinked angle of crack	k_I	Mode I global stress intensity factor
k_{II}	Mode II global stress intensity factor	k_{eq}	Equivalent local stress intensity factor
N_f	Final life	C	Paris coefficient
m	Paris coefficient	t	Sheet thickness
F	Applied load	r	Radius of weld nugget
d	Diameter of weld nugget		

1. Introduction

The Friction stir welding was invented by The Welding Institute (TWI) in 1991 as a bonding method of aluminum alloys in the solid state. Mazda Company introduced the friction stir spot welding (FSSW) in 2003. In the displacement control FSSW system, different kinds of parameters such as rotational speed, holding time in the stirring step, depth of indentation, the geometry of the pin, and shoulder and the velocity of indentation and retraction have some effects on the

quality and consequently on the mechanical behavior of friction stir spot welding (FSSW). By changing the amount of these parameters, the amount of produced heat within the process would vary, so the behavior of the welding could change [1, 2, 3]. Furthermore, one of the parameters that can affect the mechanical behavior of weld is the thickness of welding sheets. Matsoukas et al. [4] compared two thicknesses on resistance spot weld (RSW). It was shown that increase of the thickness resulted in better static and fatigue strength. Ertas et al. [5] and Rahman et al. [6] investi-

*Corresponding author: A.R. Shahani (Professor)
E-mail address: shahani@kntu.ac.ir
<http://dx.doi.org/10.22084/jrstan.2018.16884.1054>
ISSN: 2588-2597

gated the effect of sheet thickness on RSW numerically and showed thicker sheets endure more cycles than the thinner ones. However, Zhang et al. [7] showed sheet thickness had a reverse effect on the fatigue life.

In many structures, cyclic loading is the most significant factor in the structure failure, so some studies focus on the fatigue behavior of FSSW. In some of these studies, failure mechanisms of cyclic loading were one of the major scopes of the investigations [8, 9, 10]. Moreover, in some other studies the relations of fatigue behavior and the welding parameters were the main aim of the research [11, 12]. Additionally, the fatigue life estimation of FSSW has been performed in different approaches. Some studies estimate the fatigue life of the FSSW by the conventional or multi-axial fatigue relations [13, 14]. On the other hand, some studies assumed the tail of the joint as a sharp crack. These studies have used some approaches based on fracture mechanics to evaluate the fatigue life of the resistance spot welding or friction spot welding [15]. The fracture mechanics based approaches use the evaluated stress intensity factors to estimate the fatigue life of FSSW. Pook [16] determined the stress intensity factors in the lap shear configuration. Zhang [17, 18] gave the stress intensity factors in various specimen configurations.

Newman and Dowling [19] developed a fatigue life prediction model of resistance spot weld of lap shear specimens based on the global stress intensity factors of the results of Pook [16]. A crack growth approach was introduced in consideration of the local stress intensity factors and the kinked crack. Furthermore, Lin et al. [20] used different global stress intensity factors in various specimen configurations to develop a fatigue life prediction model based on local stress intensity factors of kinked cracks. The local stress intensity factors can be calculated by the global stress intensity factors and the kink angle when the kink length approaches zero [21, 22]. The developed fatigue life prediction model of Newman and Dowling [19] is based on the independency of the local stress intensity factors of resistance spot welds to the kink angle and length. Moreover, some efforts have been accomplished to calculate the local stress intensity factors based on the three-dimensional finite element analyses [23, 24, 25].

The previous studies on the effect of sheet thickness on the spot weld are limited on the resistance spot weld and few investigations were focused specifically on the observation of the sheet thickness effect on fatigue behavior of FSSW. The studies which focus on fatigue behavior were limited to the investigation of the failure modes and numerical verifications on specific welding condition. Therefore, in this work, the sheet thickness

of FSSW on Al 6061-T6, as one of the leading factors which affects the welding quality was experimentally and numerically investigated. Static strength and fatigue behavior in three different sheet thicknesses were analyzed and correlated. Finally, an optimized sheet thickness was extracted. Experimental results of different thicknesses were compared with those obtained from evaluation of numerical and theoretical models. Additionally, two different fatigue failure modes were observed at different load levels of different sheet thicknesses. The shear fracture of the welding joint and the transverse crack growth in the sheets.

2. Material and Specimen Preparation

In this investigation, Al 6061-T6 aluminum alloy in the form of a sheet with 2, 3, and 4mm thicknesses was used. Chemical composition and mechanical properties of this alloy are listed in Table 1 and Table 2, respectively [26]. Lap-shear configuration was utilized, which was made by two 40mm by 160mm sheets. Moreover, a 40mm by 40mm area was used for overlap. Two spacers with 40mm by 4mm were attached to the end of samples (Fig. 1) to eliminate misalignment and the torsional moments [27].

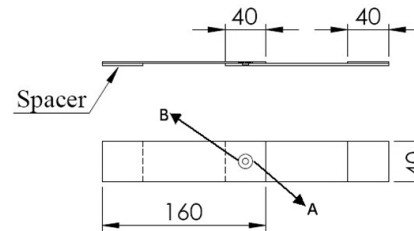


Fig. 1. Geometry of lap-shear specimens.

The welding tool was made of hot-work tool steel of H13 which was tempered and hardened to 45-48 HV [28]. Fig. 2 shows the apparatus which has 6-degree concave shoulder and conventional pin with 14mm and 6mm diameters, respectively. Vertical CNC automated machining system was used for the welding process. In displacement controled FSSW process, parameters such as rotational speed, holding time of stirring and indentation depth of the pin were introduced as the most effective parameters of the welding process, so in order to investigate the effect of holding time, the other parameters were taken constant values in all specimens. Thus, the specifications of the prepared specimens were 4 seconds of holding time, with 750rpm of rotational speed and 3, 4, and 5mm of plunge depth of 2, 3, and 4mm thicknesses, respectively. Moreover, the other effective parameters such as indentation and retraction speed were taken 10 and 100mm/min, respectively.

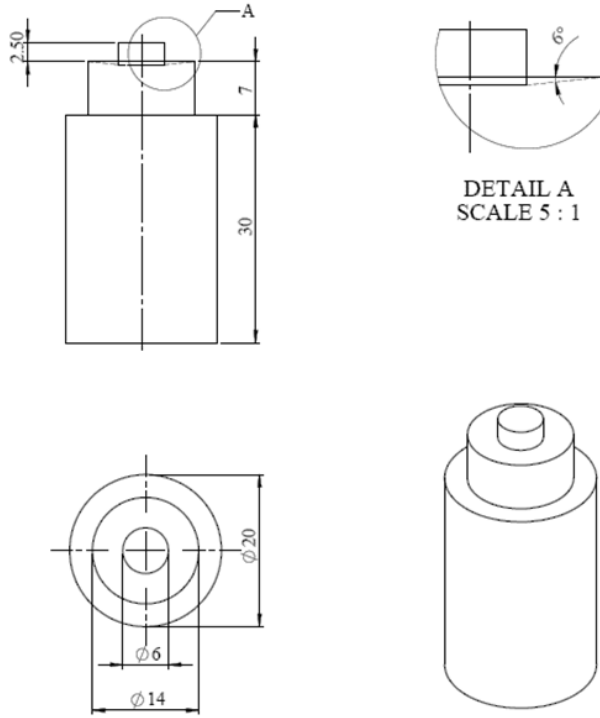
Table 1
Chemical composition of Al 6061-T6.

Element	Al	Mg	Si	Cr	Mn	Ti	Cu	Zn	Fe
Percent (%)	Bal.	0.69	0.54	0.20	0.07	0.05	0.32	0.09	0.46

Table 2

Mechanical properties of Al 6061-T6 [26].

Mechanical property	Value
Poisson's ratio	0.33
Modulus of elasticity	68.9GPa
Yield stress	276MPa
Ultimate tensile strength	310MPa

**Fig. 2.** Welding tool configuration.

3. Experimental Procedure

Tensile and fatigue experiments were performed with Zwick/Roell fatigue testing device. Static strength was determined by 2mm/min rate of loading at room temperature. The loading procedure continued until the separation of welding where load and displacement were recorded simultaneously. Fatigue experiments were performed at six different load levels with a sinusoidal stress ratio of 0.1 and frequency of 10Hz [29]. Final rupture of the joint was considered as the termination of the fatigue test.

4. Numerical Procedure

In the fatigue life prediction model of Newman and Dowling [19], which is expressed in Eq. (1) to Eq. (4), the local stress intensity factors (SIF) of the main crack can be represented by the global SIFs. The and are the global and and are the local stress intensity factors and is the kinked angle. The global stress intensity factors were calculated by the theoretical equations developed by Pook [16] and Zhang [17] in Equation (5) to Eq.

(8), respectively. In these equations F is the applied load, t is the sheet thickness and r and d are radius and diameter of weld nugget, respectively.

$$k_I = \frac{1}{4} \left(3 \cos \frac{\alpha}{2} + \cos \frac{3\alpha}{2} \right) K_I - \frac{3}{4} \left(\sin \frac{\alpha}{2} + \sin \frac{3\alpha}{2} \right) K_{II} \quad (1)$$

$$k_{II} = \frac{1}{4} \left(\sin \frac{\alpha}{2} + \sin \frac{3\alpha}{2} \right) K_I + \frac{1}{4} \left(\cos \frac{\alpha}{2} + 3 \cos \frac{3\alpha}{2} \right) K_{II} \quad (2)$$

$$k_{eq} = \sqrt{k_I^2 + k_{II}^2} \quad (3)$$

$$N_f = \frac{1}{C} \frac{t}{\sin \alpha} [\Delta k_{eq}]^{-m} \quad (4)$$

$$K_I = \frac{F}{r^{3/2}} \left[0.341 \left(\frac{2r}{t} \right)^{0.397} \right] \quad (5)$$

$$K_{II} = \frac{F}{r^{3/2}} \left[0.282 + 0.162 \left(\frac{2r}{t} \right)^{0.710} \right] \quad (6)$$

$$K_I = \frac{\sqrt{3}F}{2\pi d\sqrt{t}} \quad (7)$$

$$K_{II} = \frac{2F}{\pi d\sqrt{t}} \quad (8)$$

The later studies evaluated the SIFs by the two and three dimensional finite element models. In these studies the global SIFs were determined by numerical analysis and then fatigue life was evaluated [25, 30, 31]. The three-dimensional finite element analysis of fatigue life of FSSW was performed by ABAQUS package. Fig. 3 shows the meshing near the crack front. According to the symmetry of the model, half of the geometry was modeled with a symmetry boundary condition. According to the Newman and Dowling [19] model, the crack was assumed as a circle. The contour integral method was used for evaluation of the SIFs. The crack initiation criterion was set to maximum tangential stress. The loading and boundary conditions were applied just like the experiments. The Paris coefficients of C and m were 5.517×10^{-8} and 3.214 respectively [32].

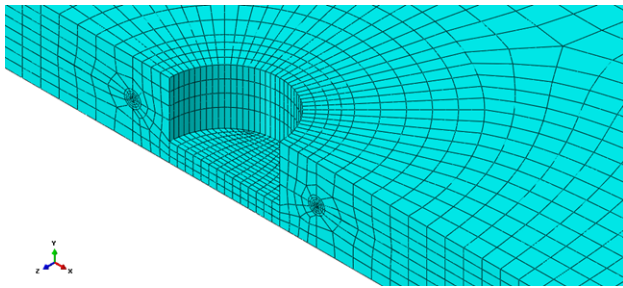


Fig. 3. Meshing of 3D finite element model.

5. Results and Discussion

The static shear strength was determined by the average of the three tested specimens for each sheet thickness. Fig. 4 compares the static strength of different welding conditions. Furthermore, Fig. 5 demonstrates the typical stress vs. strain curves of welding joints with different sheet thicknesses. It can be observed that thinner sheets show better static strength. So, the sheets with 2mm thickness show the optimum static strength.

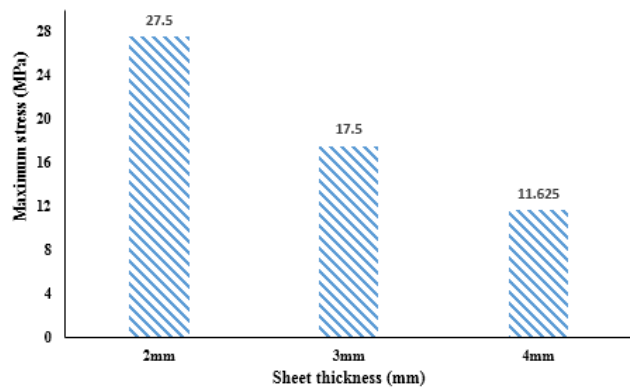


Fig. 4. Comparison of the static shear strength of different welding conditions.

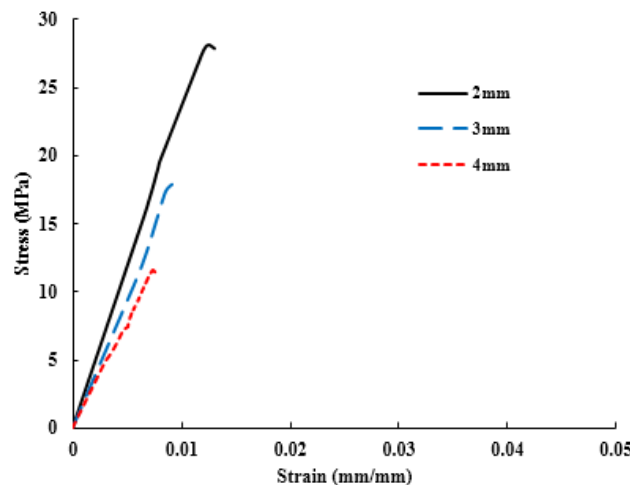


Fig. 5. Stress vs. strain curves of different welding joints.

Fatigue tests were performed and repeated at six

various load levels considering the static strength of similar welding conditions. The average life of three specimens in each load level of different welding conditions is illustrated in Fig. 6. The differences among the results of each load level is set up to 10 percent, therefore, the more difference leads to performing the extra experiments. The fatigue results reveal the fatigue strength of the FSSW increases in the thinner sheets at the same load levels. Additionally, fatigue lives between different thicknesses indicate more differences at the higher load levels, which causes steeper trend-lines. The tested sheets were produced by the rolling process, so the microstructure of the different thicknesses would be different. Therefore, the different microstructure of the specimens led to different fatigue behavior and the thinner sheet thicknesses demonstrated better fatigue lives.

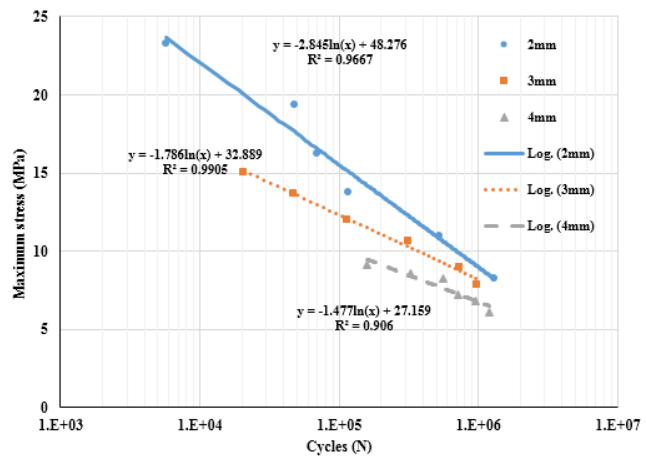
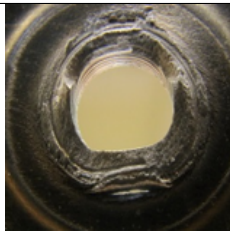
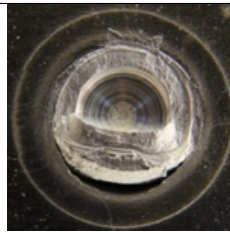
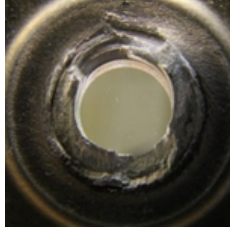
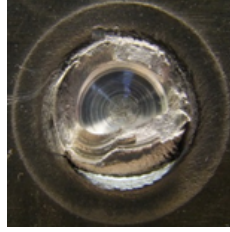
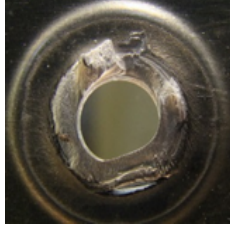

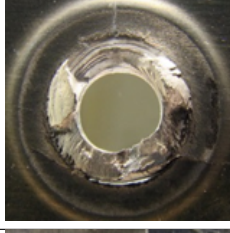

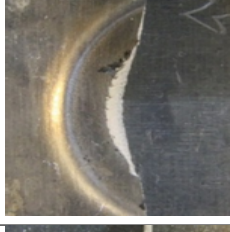





Fig. 6. Fatigue results of different welding conditions.

The failure modes of various load levels were different and are compared in Table 3. In this table, the failure surfaces of the bottom and top sheet of the 2mm thickness, as the best case of the welding process, in different load levels are illustrated in macrograph. Obviously, in the high levels, the failure mode is the shear and nugget pull-out. However, at low levels, the failure mode is the transverse crack growth. However, for the all tested specimens with 3 and 4mm thicknesses the only occurred fatigue failure mode was the shear one. The failure process was initiated by a kinked crack and the final rupture occurred by the nugget pull-out or shear fracture.

At the same cycles, fatigue behavior of different welding conditions shows higher differences in the lower cycles than the higher ones. The discussed behavior can be justified by the different failure modes of specimens at the lower and higher load levels. The different failure mode of 2mm thickness at low load levels caused the steeper slope. Furthermore, the 3 and 4mm thicknesses had more similar slopes which can be a consequence of the same failure mode at the all different load levels.

Table 3
Comparison of failure surfaces under different load levels of 2mm thickness.

Maximum load (kN)	Ratio of static strength (%)	Failure surface of welding	
		Top sheet	Bottom sheet
3.73	85		
3.1	70		
2.6	60		
2.2	50		
1.76	40		
1.32	30		

The elements of the numerical model were the quadratic three-dimensional stress elements with 20 nodes and reduced integration formulation (C320DR). The mesh refinement and convergence were accomplished. Fig. 7 illustrates the mesh convergence of the finite element model on the crack front. The crack front is the most critical region of this model. So, the size of 0.4mm was chosen as the refined size of the el-

ements on the crack front. Moreover, the regions far from the crack zone were meshed with the elements of 0.8mm sizes. Therefore, the numerical model was constructed by 30500 elements. The distribution of the stress intensity factors through the crack front are illustrated in the Fig. 8. So, the maximum equivalent stress intensity factor of the crack front occurred at 0 and 180 degrees (the specified points A and B in the

Figure 1). Fig. 9 to Fig. 11 compare the evaluated life of the different models with experimental results in different thicknesses. It can be observed that Zhang [17] and three-dimensional finite element models overestimate the fatigue life at all load levels. However, Pook [16] model overestimates the fatigue life at high load levels and underestimates it at low load levels. Additionally, the differences of Zhang [17] and Pook [16] models grow bigger with increasing the thickness.

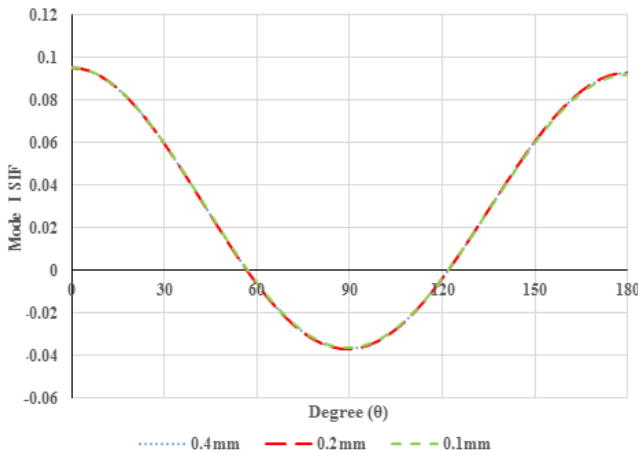


Fig. 7. Mesh convergence of the model on the crack front.

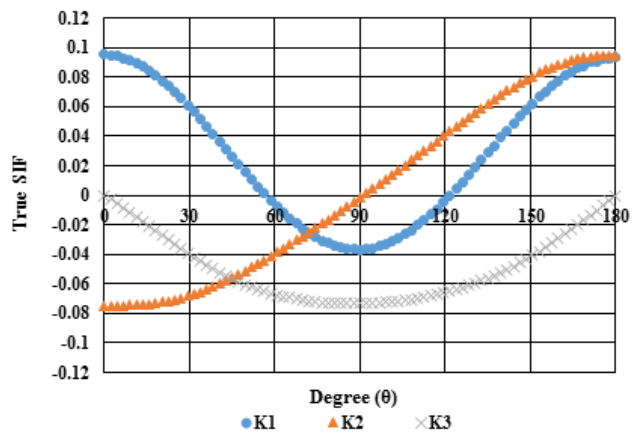


Fig. 8. Distribution of stress intensity factors through the crack front of 1N load.

The FEM model got more details of the specimens to evaluate the SIFs than the two theoretical models. The theoretical models were also developed on the resistance spot welding; however, friction spot welding was investigated in this work. The friction stir spot welding and resistance spot welding were totally different in geometric point of view. The key hole of the stirring process and other geometrical parameters of the friction stir spot welding were not considered in the theoretical models. So, the results showed that the three-dimensional FEM evaluates the fatigue life better than the other models. More load levels were also underestimated by Pook [16] model in the thicker sheets.

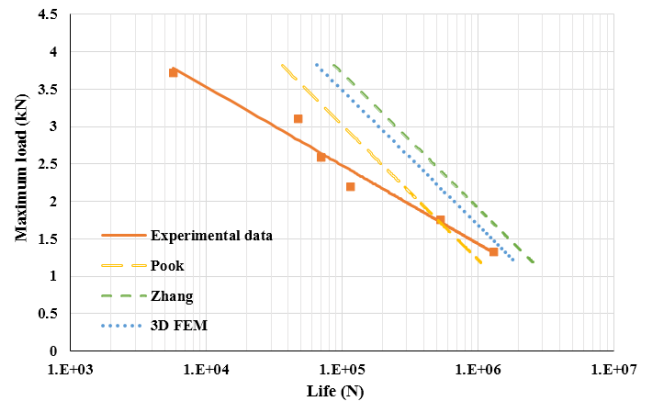


Fig. 9. Comparison of experimental and numerical results of 2mm.

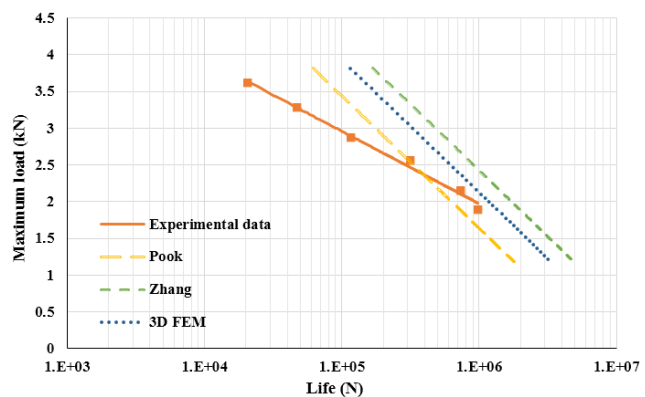


Fig. 10. Comparison of experimental and numerical results of 3mm.

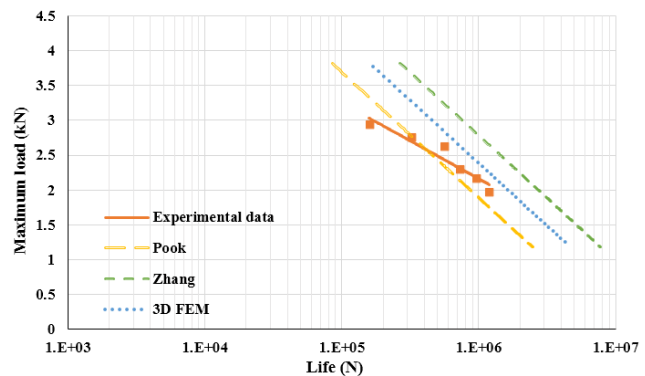


Fig. 11. Comparison of experimental and numerical results of 4mm.

6. Conclusions

Static strength and fatigue behavior of friction stir spot weld of Al 6061-T6 alloy in the different sheet thicknesses were investigated experimentally.

Different fatigue life evaluation models were applied to estimate the fatigue behavior of the FSSW in different thicknesses.

Experimental results showed a clear correlation between static strength and fatigue behavior of different welding conditions. Results of tensile and fatigue tests

demonstrated the sheets with 2mm were the optimum welding conditions which was studied in this research. At the same cycles, fatigue results of different welding conditions showed considerable differences in the low cycles in comparison with the higher ones.

The evaluation models of Pook [16], Zhang [17] and three-dimensional finite element models were investigated in different sheet thicknesses. The 3D FEM and Zhang [17] models overestimated the fatigue life at all load levels. Pook [16] model overestimated the fatigue life at high load levels and underestimated at low load levels. Pook [16] model underestimated thicker sheets more than the thinner sheets. The three-dimensional finite element model evaluated fatigue behavior better than the two other models at different sheet thicknesses.

References

- [1] T. Rosendo, B. Parra, M.A.D. Tier, A.A.M. Da Silva, J.F. Dos Santos, T.R. Strohaecker, N.G. Alcântara, Mechanical and microstructural investigation of friction spot welded AA6181-T4 aluminium alloy, *Mater. Des.*, 32(3) (2011) 1094-1100.
- [2] Z. Zhang, X. Yang, J. Zhang, G. Zhou, X. Xu, B. Zou, Effect of welding parameters on microstructure and mechanical properties of friction stir spot welded 5052 aluminum alloy, *Mater. Des.*, 32(8-9) (2011) 4461-4470.
- [3] Y. Tozaki, Y. Uematsu, K. Tokaji, Effect of processing parameters on static strength of dissimilar friction stir spot welds between different aluminium alloys, *Fatigue. Fract. Eng. Mater. Struct.*, 30(2) (2007) 143-148.
- [4] G. Matsoukas, G.P. Steven, Y.W. Mai, Fatigue of spot-welded lap joints, *Int. J. Fatigue.*, 6(1) (1984) 55-57.
- [5] A.H. Ertas, F.Q. Sonmez, A parametric study on fatigue strength of spot-weld joints, *Fatigue. Fract. Eng. Mater. Struct.*, 31(9) (2008) 766-776.
- [6] M.M. Rahman, R.A. Bakar, M.M. Noor, M.R.M. Rejab, M.S.M. Sani, M.S.M., Fatigue life prediction of spot-welded structures: a finite element analysis approach, *Eur. J. Sci. Res.*, 22(3) (2008) 444-456.
- [7] Y. Zhang, D. Taylor, Sheet thickness effect of spot welds based on crack propagation, *Eng. Fract. Mech.*, 67(1) (2000) 55-63.
- [8] P.C. Lin, Z.M. Su, R.Y. He, Z.L. Lin, Failure modes and fatigue life estimations of spot friction welds in cross-tension specimens of aluminum 6061-T6 sheets, *Int. J. Fatigue.*, 38 (2012) 25-35.
- [9] Z.M. Su, R.Y. He, P.C. Lin, K. Dong, Fatigue analyses for swept friction stir spot welds in lap-shear specimens of alclad 2024-T3 aluminum sheets, *Int. J. Fatigue.*, 61 (2014) 129-140.
- [10] V.X. Tran, J. Pan, Fatigue behavior of dissimilar spot friction welds in lap-shear and cross-tension specimens of aluminum and steel sheets, *Int. J. Fatigue.*, 32(7) (2010) 1167-1179.
- [11] H.M. Rao, J.B. Jordon, M.E. Barkey, Y.B. Guo, X. Su, H. Badarinarayan, Influence of structural integrity on fatigue behavior of friction stir spot welded AZ31 Mg alloy, *Mater. Sci. Eng. A*, 564 (2013) 369-380.
- [12] A.M.S. Malafaia, M.T. Milan, M.F. Oliveira, D. Spinelli, Fatigue behavior of friction stir spot welding and riveted joints in an Al alloy, *Procedia. Eng.*, 2(1) (2010) 1815-1821.
- [13] S.R. Ahmadi, S. Hassanifard, M.M. Pour, Fatigue life prediction of friction stir spot welds based on cyclic strain range with hardness distribution and finite element analysis, *Acta Mech.*, 223(4) (2012) 829-839.
- [14] A.H. Ertas, F.O. Sonmez, Design optimization of spot-welded plates of maximum fatigue life, *Finite Elem. Anal. Des.*, 47(7) (2011) 413-423.
- [15] P.C. Lin, J. Pan, T. Pan, Failure modes and fatigue life estimations of spot friction welds in lap-shear specimens of aluminum 6111-T4 sheets. Part 2: Welds made by a flat tool, *Int. J. Fatigue.*, 30(1) (2008) 90-105.
- [16] L.P. Pook, Fracture mechanics analysis of the fatigue behaviour of spot welds, *Int. J. Fract.*, 11(1) (1975) 173-176.
- [17] S. Zhang, Stress intensities at spot welds, *Int. J. Fract.*, 88(2) (1997) 167-185.
- [18] S. Zhang, Fracture mechanics solutions to spot welds, *Int. J. Fract.*, 112(3) (2001) 247-274.
- [19] J.A. Newman, N.E. Dowling, A crack growth approach to life prediction of spot-welded lap joints, *Fatigue. Fract. Eng. Mater. Struct.*, 21(9) (1998) 1123-1132.
- [20] S.H. Lin, J. Pan, P. Wung, J. Chiang, J., A fatigue crack growth model for spot welds under cyclic loading conditions, *Int. J. Fatigue.*, 28(7) (2006) 792-803.
- [21] B.A. Bilby, G.E. Cardew, I.C. Howard, Stress intensity factors at the tips of kinked and forked cracks, *Anal. Mech.*, 3 (1978) 197-200.
- [22] B. Cotterell, J. Rice, Slightly curved or kinked cracks, *Int. J. Fract.*, 16(2) (1980) 155-169.

- [23] D.A. Wang, S.H. Lin, J. Pan, Stress intensity factors for spot welds and associated kinked cracks in cup specimens, *Int. J. Fatigue.*, 27(5) (2005) 581-598.
- [24] N. Pan, S.D. Sheppard, Stress intensity factors in spot welds, *Eng. Fract. Mech.*, 70(5) (2002) 671-684.
- [25] D.A. Wang, J. Pan, A computational study of local stress intensity factor solutions for kinked cracks near spot welds in lap-shear specimens, *Int. J. Solids. Struct.*, 42(24-25) (2005) 6277-6298.
- [26] ASM Handbook, Properties and Selection: Non-ferrous Alloys and Special-Purpose Materials, ASM International 2 (1990).
- [27] SAE. Welding: Resistance, Spot and Seam, AMS-W 6858. Pennsylvania, USA: SAE, (1999).
- [28] ASM Handbook, Heat Treating. ASM International, 4 (1991).
- [29] ISO14324, Resistance Spot Welding–Destructive Tests of Welds-Method for the Fatigue Testing of Spot Welded Joints. The International Organization for Standardization, (2003).
- [30] D.A. Wang, C.H. Chen, Fatigue lives of friction stir spot welds in aluminum 6061-T6 sheets, *J. Mater. Proces. Tech.*, 209(1) (2009) 367-375.
- [31] D.A. Wang, P.C. Lin, J. Pan, Geometric functions of stress intensity factor solutions for spot welds in lap-shear specimens, *Int. J. Solid. Struct.*, 42(24-25) (2005) 6299-6318.
- [32] B.F. Jogi, P.K. Brahmankar, V.S. Nanda, R.C. Prasad, Some studies on fatigue crack growth rate of aluminum alloy 6061, *J. Mater. Process. Technol.*, 201(1-3) (2008) 380-384.